Fermi National Accelerator Laboratory

FERMILAB-Pub-79/34-EXP
7310.025

MEASUREMENTS OF ELASTIC RHO AND PHI MESON PHOTOPRODUCTION CROSS SECTIONS ON PROTONS FROM 30 TO 180 GeV

R. M. Egloff, P. J. Davis, G. J. Luste
J. F. Martin and J. D. Prentice
University of Toronto
Toronto, Ontario M5S1A7, Canada

and

D. O. Caldwell, J. P. Cumalat, A. M. Eisner, A. Lu,
R. J. Morrison and S. J. Yellin
University of California
Santa Barbara, California 93106

and

T. Nash
Fermi National Accelerator Laboratory
Batavia, Illinois 60510

May 1979

MEASUREMENTS OF ELASTIC RHO AND PHI MESON PHOTOPRODUCTION CROSS SECTIONS ON PROTONS FROM 30 TO 180 GeV

R. M. Egloff, P. J. Davis, G. J. Luste
J. F. Martin and J. D. Prentice
University of Toronto
Toronto, Ontario M5S1A7, Canada

and

D. O. Caldwell, J. P. Cumalat,[a] A. M. Eisner, A. Lu,
R. J. Morrison and S. J. Yellin
University of California
Santa Barbara, California 93106

and

T. Nash
Fermi National Accelerator Laboratory
Batavia, Illinois 60510

The elastic photoproduction cross sections for rho and phi mesons from protons have been measured from 30 GeV to 180 GeV. The energy dependences agree well with predictions made by using vector meson dominance and an additive quark model. The rho cross section is approximately constant with energy while the phi cross section rises from 0.5 μb to 0.7 μb with increasing energy.

In this paper we present results on the elastic photoproduction of rho and phi mesons on protons, $\gamma p \to \rho^0 p$ and $\gamma p \to \phi p$. The decay modes we observed were $\rho^0 \to \pi^+\pi^-$ and $\phi \to K^+K^-$. The data were taken during the photon total cross section experiment[1] at the Tagged Photon Laboratory of Fermilab.

A schematic diagram of the apparatus is shown in Fig. 1. The hydrogen target is 1 meter long and is surrounded by four scintillation recoil counters. The detectors S1 and S2 are multilayer lead-iron-scintillation counters; S3 and K are iron-scintillator hadrometers; G2 and G3 are lead glass shower counter arrays; and C and D are lead-scintillator shower detectors. In front of the G3 lead glass array are six multiwire proportional chambers (MWPC's). More details on the detection apparatus can be found in Ref. 1.

Since the apparatus did not have a magnet or a Cerenkov counter, we were unable to measure mass spectra directly or to discriminate between pions and kaons for ρ^0 and ϕ meson production. However, our full coverage of the forward hemisphere in the γp center-of-mass frame allowed us to select events with exactly two tracks, and no extra particles in S1, S2, S3, or G3. The opening angle multiplied by the two-track energy (assumed equal to the tagged photon energy) provided an excellent substitute for the actual invariant mass, in that the ρ^0 and ϕ decays show up as two distinct peaks.

Consider now the elastic production of a short-lived meson, mass M and energy E (we neglect the recoil kinetic energy), which decays into two particles of mass $m \neq 0$. For $E \gg M$, the track

separation, Δ, can be written to an excellent approximation as

$$\Delta = \frac{4Z \sin\theta \sqrt{\left(\frac{M}{2}\right)^2 - m^2}}{E \left\{ \sin^2\theta + \left(\frac{2m}{M}\right)^2 \cos^2\theta \right\}} \qquad (1)$$

where θ is the decay angle in the rest frame of M, and Z is the distance from the target to the position where Δ is measured.

When Eq. (1) is evaluated for the decay $\phi \to K^+K^-$, the maximum track separation is $\Delta\phi_{max} = .509\ Z/E$, whereas nearly all ρ^o decays at $M = M_\rho$ (770) have $\Delta \geq 1.432\ Z/E$ (the value for $\theta = 90^o$). From Eq. (1) we note that the distribution of $E\Delta$, or, more conveniently, $R \equiv \Delta/\Delta\phi_{max}$ is independent of E. This makes it possible to plot a combined R-spectrum for the entire tagging range (E = 45 to 92% of the electron beam energy, E_o).

Only events which satisfied certain criteria were included in the R distribution. An event was considered an elastic candidate if the event had exactly two tracks in the MWPC's and if more than 35% of the tagged photon energy, E_γ, was contained in H3 (see Fig. 1). Next, all signals in G3 were required to be associated with tracks, and the upstream detectors, S1, S2 and G2, were used as veto counters. Finally, electromagnetic pairs were excluded by requiring the energy in G3 and C to be less than 60% of E_γ. The R-distribution for E_o = 90 GeV is shown in Fig. 2a.

In order to extract ρ^o and ϕ yields from data plots like Fig. 2a, a Monte Carlo program was used to produce expected R distributions. Assuming s-channel helicity conservation[2] and hence, a

$\sin^2\theta$ decay distribution, R spectra for ρ^o and ϕ decays were generated using the known photon spectrum. The Monte Carlo calculation folded in the rho mass shape, geometrical acceptance, target length, beam size, and resolution in photon energy and in Δ. Cross sections are assumed to vary with t (t = four momentum transfer squared) like e^{bt} with $b(\rho) = 8.5\ \text{GeV}^{-2}$ and $b(\phi) = 6.5\ \text{GeV}^{-2}$. Results were insensitive to uncertainties in these numbers aside from a weak dependence of the rho acceptance on $b(\rho)$.

The ρ mass spectrum requires further discussion. We have used the Söding parameterization[3,4] of a ρ interfering with a non-resonant background:

$$\frac{dN}{dM} = \frac{C_o M M_\rho \Gamma}{(M^2-M_\rho^2)^2 + M_\rho^2 \Gamma^2} \left\{1 + C_1\left(\frac{M_\rho^2}{M^2} - 1\right) + C_2\left(\frac{M_\rho^2}{M^2} - 1\right)^2\right\} \quad (2)$$

with $M_\rho = 0.773$ GeV and a mass-dependent width[5]

$$\Gamma = \left(\frac{q(M)}{q(M_\rho)}\right)^3 \frac{2\Gamma_o}{1 + \left[q(M)/q(M_\rho)\right]^2} \quad (3)$$

Here $\Gamma_o = 0.150$ GeV, and q(M) is the magnitude of the 3-momentum in the π-π center of mass frame. The ρ^o yield is then defined to equal $\frac{\pi}{2} C_o$.[4]

Two additional processes have been included. The decay $\phi \to K_L^o K_S^o \to K_L^o \pi^+\pi^-$ has been computed to contribute less than 1% to the ρ; it is shown in Fig. 2a. There is also a small low R contribution surviving our cuts from Bethe-Heitler e^+e^- pairs in which one member has interacted hadronically in C or G3. Their R-

dependence was obtained from non-interacting pairs, but the normalization (N_{ee}) left free. Using the R spectra for all contributions, five-parameter fits were done to determine C_o, C_1, C_2, the ϕ yield, and N_{ee}. Good fits were obtained for all data points, giving average C_1 and C_2 values of 3.0 ± 0.7 and 2.0 ± 0.5. The total ρ and e^+e^- contributions for the 90 GeV electron energy setting are drawn in Fig. 2a. Figure 2b shows the ϕ data (summed over all data points) with all other processes subtracted; also shown are predicted R spectra assuming s-channel helicity conservation (solid line) and, for comparison, isotropic decay (dotted line).

Corrections to the ρ^o and ϕ yields were applied for geometric acceptance (the acceptance determined by the Monte Carlo program averaged 60% for the ρ and 96% for the ϕ), two-track reconstruction inefficiency (9%), inelastic π or K interactions between production and chambers (15% and 11%), decays in flight (averaging 1% and 7%), events lost by analysis cuts (4% and 4%), and the ϕ branching ratio to K^+K^- (46.6%).

We also corrected for contamination from inelastic events involving target dissociation with no downstream products. Elastic and inelastic events could be statistically distinguished by their different probabilities for firing n of the 4 recoil counters. Diffractive events have $n \leq 1$, usually $n = 0$, with probabilities computable from range-energy relations. Inelastic events almost always have $n \geq 1$, usually $n > 1$. Probabilities were estimated by a simple Poisson model which agrees with hadronic studies of target

dissociation,[6] but our results are not very sensitive to details of the model. The inelastic events eliminated amounted to 13% for the ρ^o, and 18% for the ϕ.

The resulting cross sections are presented in Table I and are shown in Fig. 3 and Fig. 4, along with results of previous experiments.[2,7-12] The quoted errors are statistical and include uncertainties due to background subtraction. The total energy-independent systematic uncertainties are estimated to be less than 5%. For the ρ there is an additional 5% systematic uncertainty due to geometrical acceptance. The curve in Fig. 4 is from a parameterization of all the data[13] and shows a rising cross section with increasing energy.

In vector meson dominance (VMD) models, the photoproduction of a vector meson, V, is related to Vp scattering. The Vp scattering can in turn be related by additive quark model relations to measured hadron processes. If we assume that the VMD and quark model relations apply to amplitudes at fixed s and t, then one can "predict" photoproduction cross sections in terms of hadronic elastic scattering cross sections:

$$\frac{d\sigma}{dt}(\gamma p \to \rho^o p) = \frac{e^2}{4\gamma_\rho^2}\left[\frac{p^*_\pi}{2p^*_\gamma}\left\{\sqrt{\frac{d\sigma}{dt}(\pi^+ p)} + \sqrt{\frac{d\sigma}{dt}(\pi^- p)}\right\}\right]^2 \qquad (4a)$$

$$\frac{d\sigma}{dt}(\gamma p \to \phi p) = \frac{e^2}{4\gamma_\phi^2}\,\frac{1}{(p^*_\gamma)^2}\left[p^*_K\left\{\sqrt{\frac{d\sigma}{dt}(K^+ p)} + \sqrt{\frac{d\sigma}{dt}(K^- p)}\right\} - p^*_\pi\sqrt{\frac{d\sigma}{dt}(\pi^- p)}\right]^2 \qquad (4b)$$

where p_x^* is the 3-momentum of x in the xp center-of-mass frame, and everything is to be evaluated at the same s. For our purposes the integral of (4a) is well-approximated by

$$\sigma(\gamma p \to \rho^o p) = \frac{e^2}{4\gamma_\rho^2} \frac{1}{2} \left[\sigma(\pi^+ p \to \pi^+ p) + \sigma(\pi^- p \to \pi^- p)\right] \qquad (5)$$

This formula is plotted in Fig. 3, using smoothed πp measurements[14-16] and $\gamma_\rho^2/4\pi = 0.64$[17], and is seen to represent the photoproduction data well.

For the ϕ, we have used forward hadron-beam data[14-16] and assumed an e^{bt} form for the photoproduction cross section with $b(s) = 4.66 + 0.38 \ln s$.[12] The resulting predictions, normalized to our ϕ data, are shown in Fig. 5 along with the curve from Fig. 4. The energy dependence is similar; the measured value of $\gamma_\phi^2/4\pi = 4.7 \pm 0.3$ resulting from the normalization is consistent with the value of 5.5 ± 2.4[17] obtained from a photoproduction experiment on complex nuclei. A value of 2.83 ± 0.2[17] is obtained from colliding beam measurements. We conclude that the energy dependence of the ϕ p elastic cross section extracted from hadronic data (using the quark model) and from photoproduction (using VMD) are in agreement.

We gratefully acknowledge support from the Fermilab staff, especially the Proton and Physics Departments and the Hydrogen Target group. We thank F. Murphy who participated in the early stages of the experiment. We also thank our technical support personnel, including M. Armstrong, D. Briggs, Y. Chan, A. Kiang, H. Nickel, D. Simmen, and R. Stuber, and students, J. Gallet and C.

Lauer. Valuable assistance was provided by M. Franklin and M. G. Donnelly, and also by A. Belousov and B. Govorkov of the Lebedev Physical Institute. This research was supported in part by the U.S. Department of Energy and by the National Research Council of Canada through the Institute of Particle Physics of Canada.

REFERENCES

[a]Present address: Fermi National Accelerator Laboratory
Batavia, Illinois 60510

[1]D. O. Caldwell et al., Phys. Rev. Lett. 40, 1222 (1978).
J. P. Cumalat, thesis, University of California, Santa Barbara, 1977 (unpublished).

[2]J. Ballam et al., Phys. Rev. D7, 3150 (1973).

[3]P. Söding, Phys. Lett. 19, 702 (1965).

[4]R. Spital and D. R. Yennie, Phys. Rev. D9, 126 (1974).

[5]J. D. Jackson, Nuovo Cimento, 34, 1644 (1964).

[6]J. Whitmore, Physics Reports 10, 273 (1974).

[7]ABBHHM Collaboration (DESY), Phys. Rev. 175, 1669 (1968).

[8]R. Anderson et al., Phys. Rev. D1, 27 (1970).

[9]W. R. Francis et al., Phys. Rev. 38, 633 (1977).

[10]C. Berger et al., Phys. Lett. 39B, 659 (1972).

[11]H. J. Besch et al., Nucl Phys. B70, 257 (1974).

[12]H. J. Behrend et al., Nucl. Phys. B144, 22 (1978).

[13]The curve is given by $\sigma = (p^*_\phi/p^*_\gamma)^2 (a + b/\sqrt{s} + c \ln s)$ with $a = -0.10 \pm 0.33$, $b = 0.94 \pm 0.64$, $c = 0.14 \pm 0.06$, σ in μb and s in GeV^2.

[14]D. S. Ayres et al., Phys. Rev. D15, 3105 (1977).

[15]K. J. Foley et al., Phys. Rev. Lett. 9, 425 (1963).

[16]I. Ambats et al., Phys. Rev. D9, 1179 (1974).

[17]D. W. G. S. Leith in Electromagnetic Interactions of Hadrons, ed. A. Donnachie and G. Shaw, Plenum Publishing Corp. (1978).

TABLE I

The Cross Section with Statistical Uncertainties for

$\gamma p \to \rho^{o} p$ and $\gamma p \to \phi p$

E_o (GeV)	E_γ (GeV)	$\sigma_{\gamma \to \rho^o} \pm \Delta\sigma$ (μb)	$\sigma_{\gamma \to \phi} \pm \Delta\sigma$ (μb)
60	35 ± 5	8.84 ± 0.44	0.506 ± .090
60*	42 ±12	10.68 ± 0.67	0.568 ± .091
60	47 ± 7	9.90 ± 0.49	0.546 ± .089
90	53 ± 7	9.50 ± 0.56	0.625 ± .063
90	71 ±11	9.82 ± 0.56	0.646 ± .065
135	79 ±11	8.24 ± 0.47	0.648 ± .052
135	106 ±16	9.22 ± 0.52	0.661 ± .053
200	117 ±17	8.59 ± 0.49	0.630 ± .101
200	157 ±23	9.75 ± 0.56	0.740 ± .092

*Data taken at a modified geometry

FIGURE CAPTIONS

Fig. 1: Schematic diagram of apparatus.

Fig. 2: R distribution for E_o = 90 GeV data is shown in (a). The various curves in (a) are explained in the text. In (b) the ϕ signal above background summed over all data points is plotted.

Fig. 3: Energy dependence of the ρ^o photoproduction cross section.

Fig. 4: Energy dependence of the ϕ photoproduction cross section. Dashed line is a parameterization of the cross section.

Fig. 5: VMD - quark model cross section normalized to the phi data of this experiment. The curve is the same as in Fig. 4.

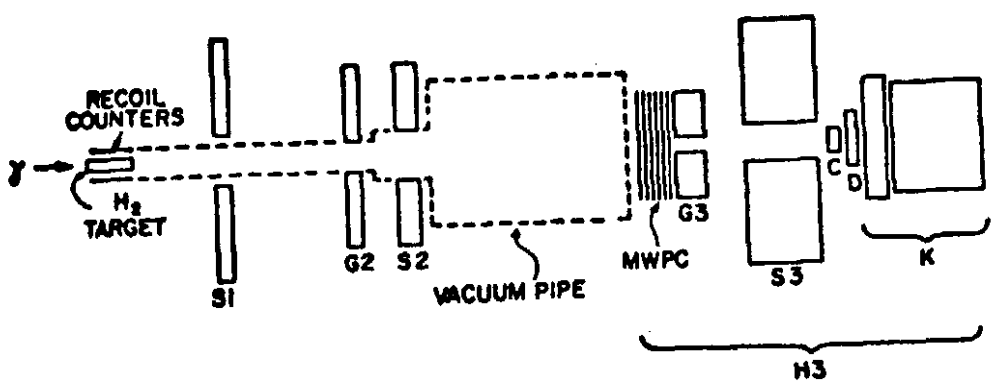
RECOIL COUNTERS
γ
H_2 TARGET
S1
G2
S2
VACUUM PIPE
MWPC
G3
S3
C
D
K
H3

FIGURE 1

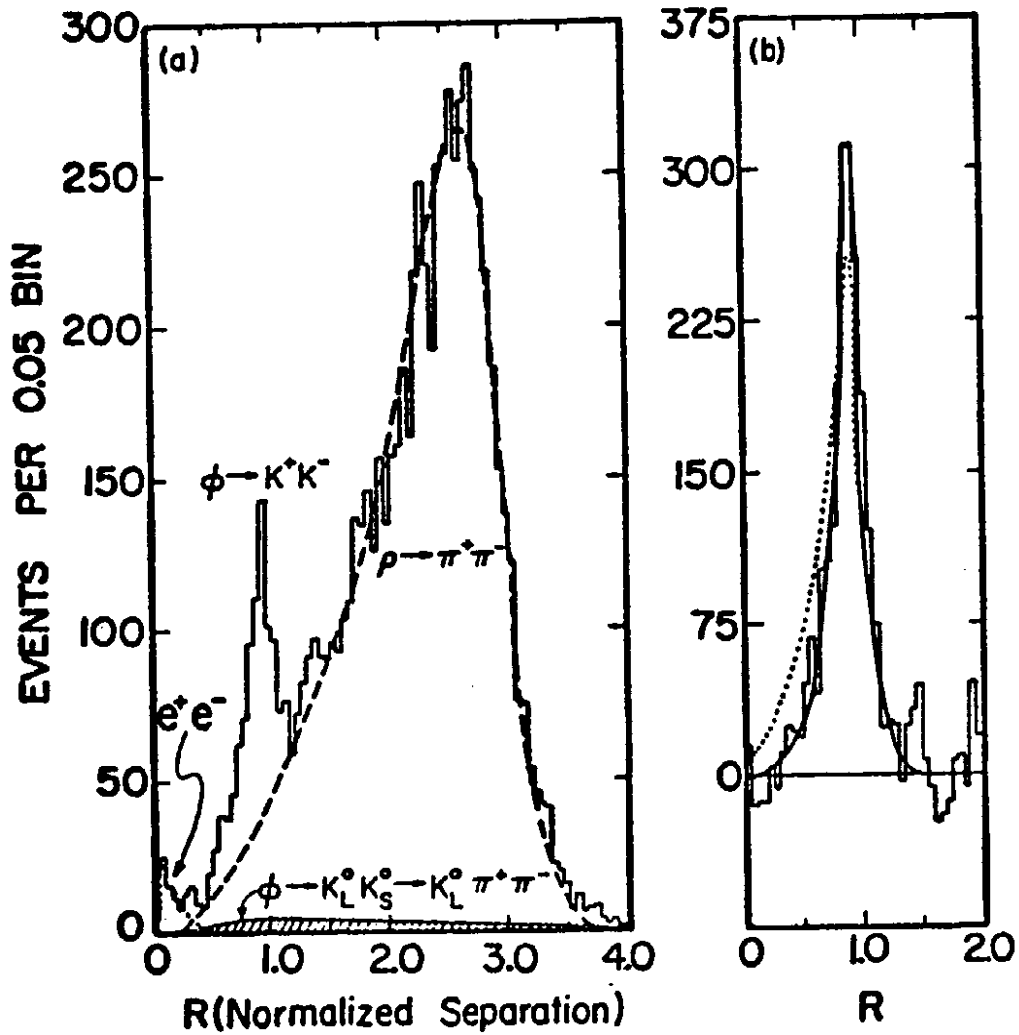
(a)
(b)
EVENTS PER 0.05 BIN
R(Normalized Separation)
R
$\phi \to K^+K^-$
$\rho \to \pi^+\pi^-$
e^+e^-
$\phi \to K_L^0 K_S^0 \to K_L^0 \pi^+\pi^-$
300
250
200
150
100
50
0
375
300
225
150
75
0
1.0
2.0
3.0
4.0

FIGURE 2

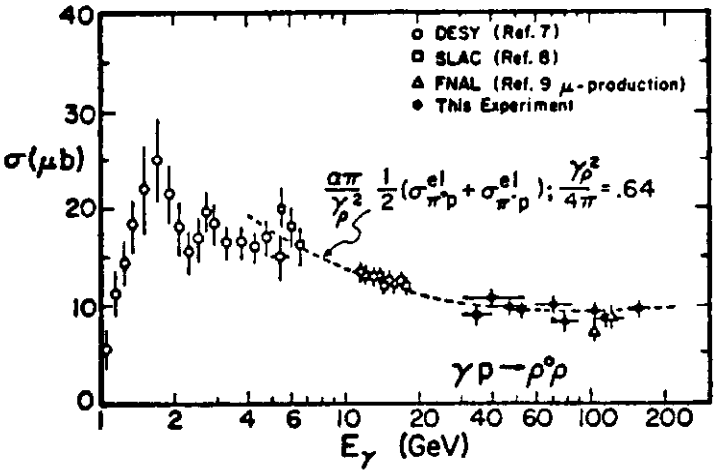

FIG. 3

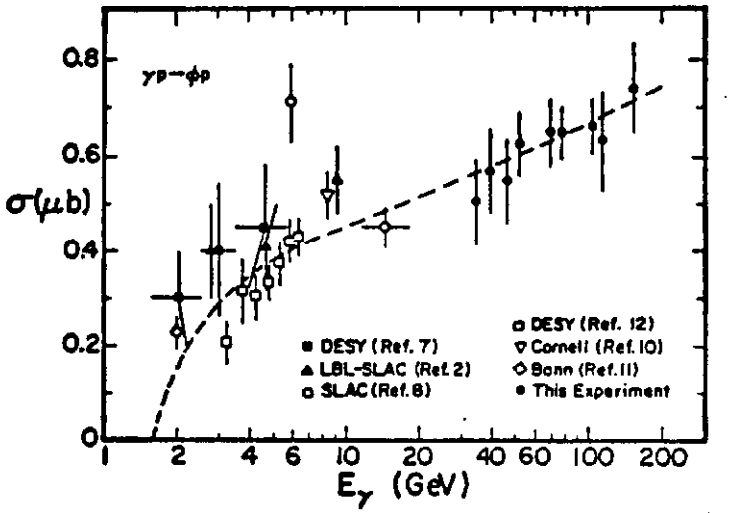

FIG. 4

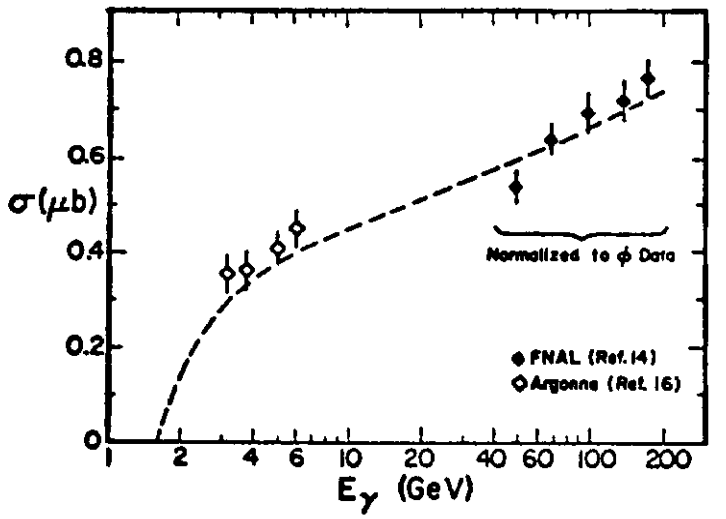

FIG. 5